

**PEG-ON-HOLE: PATTERNS OF MOTION
TO ENSURE ALIGNMENT OF PEG WITH
VERTICALLY FIXED HOLE DURING AUTOMATED ASSEMBLY**

Ludmila B. Chernyakhovskaya

Candidate of Physico-mathematical Sciences

Samara State Technical University

tms@samgtu.ru

Dmitry A. Simakov

Doctor of Natural Science, Independent Researcher

dmsimak@gmail.com

Abstract. Automation of assembling cylindrical parts is a currently central problem of the technology of machine-building. To address it, assembly devices shall be improved, and software programs for controlling alignment process shall be created. The ways of improving cylindrical parts assembly operations depend on whether movement of an actuator is in compliance with the objectively defined laws of motion that specify the process of alignment. The paper is aimed at studying peg-on-hole motion supported at the edge of vertically fixed hole, and creating thereupon a mathematical model for the process of aligning cylindrical parts. The task set was tackled using methods of theoretical mechanics. They enabled to identify common patterns of peg motion with three degrees of freedom and involving planar motion that facilitates the process of aligning parts when nutation angle changes, rotational motion around hole axis characterized with precession angle, and rotational motion about its axis defined by self-rotation angle. The analysis conducted enabled to find directions of velocities, normal reactions, and friction forces at the contact points. A system of differential equations in generalized coordinates, which we call Dynamic Differential Equations, is created. It is a mathematical model describing the process of aligning cylindrical parts in general terms, and allowing to analyze all possible alternatives of vertical assembly. A particular case of this motion is analyzed when peg has two degrees of freedom performing planar motion and rotating about its axis. It is found that here the forces acting on the peg at the contact points shall be considerably reduced that improves the conditions for alignment of parts and quality of assembly as well. The equations of one freedom degree motion of a peg served as a basis for developing a method of experimental determination of friction coefficient for assembling certain parts which improves accuracy of finding interaction forces. The results obtained are of practical importance when evaluating and developing methods for assembling, designing assembly devices, imply the ways to improve assembly operations, develop software programs and train Artificial Intelligence for controlling assembly process.

Key words: cylindrical parts, three contact points, compound motion, three degrees of freedom, dynamic responses, differential equations.

Introduction

Assembly of cylindrical connections like Peg-in-Hole in machine-building industry may amount to about 20%, and in instrument-making industry – up to 40% of all assembly operations. Therefore, automation of the process is a relevant task, for which robotic systems have increasingly been in use to cope with. Design and development of assembly devices classically involves an advanced computer modelling of automatic assembly of cylindrical parts. In addition, the rapidly developed Artificial Intelligence (AI) methods can be trained to perform the same tasks in a more intelligent way. The need in assembly devices for Peg-in-Hole configuration increases the importance of knowledge of the analytical model for the patterns of mechanical motion. In classical programming this knowledge increases the calculation speed and the quality of the result. For AI, this knowledge eases the task of the training, and increases its precision. Therefore, a detailed study of alignment process using methods of theoretical mechanics is still of a great importance and will take its new niche in the digital era.

Most known methods and devices intended to automatically assemble cylindrical parts with a minimum clearance imply alignment schemes with a vertically fixed hole and a movable peg. Alignment of parts starts with the initial contact of the parts at two or three points. The position of the peg in both cases is characterized with the three Euler angles, the generalized coordinates. It means, the peg is able to make three motions independently from one another: (i) axial rotation characterized with self-rotation angle φ ; (ii) rotation around peg axis, defined by precession angle ψ , and (iii) planar motion characterized by nutation angle γ between axes of the parts. Both rotating motions have no effect on movement of the peg inside the hole. The process of alignment takes place as a planar motion with reduction of angle γ . However, it does not mean that rotating motions of the peg do not have any effect on the alignment process as such.

The analytical problems of vertical scheme for assembling cylindrical parts have been addressed in many research papers. The common patterns of planar motion were defined to ensure alignment of the parts, and the reasons for their damage or seizure were found. A rather complete analysis of the alignment process with two-point contact between the parts has been carried out. The required geometrical and kinematic characteristics, and force interactions between a peg and a hole at the contact points were defined for this process in [1] and [2] depending on angle γ between the axes. Alternatives for relative orientation of the parts during automatic assembly were considered in [3-6], and criteria for recognizing them were specified. Many studies are devoted to analysis of the peg movement supported at the three points of the hole aperture edge, a so-called three-point contact. Directions of all interaction forces in this case were defined, and trajectories of all peg points and velocities of the contact were determined in [7-10]; differential equations of the peg motion characterizing alignment process were made [11]. The reasons of the parts' seizure were consid-

ered in detail, including action of gravity on the movable part producing considerable forces of interaction between a peg and a hole at the contact points. A potential reduction of this effect was analyzed through changing the position of the center of gravity of the movable part [12], [13].

To improve efficiency of automated assembly of cylindrical parts, robotic systems have increasingly been in use to control the process with software programs developed based on real experiment with the elements of AI training [14], [15], [17], [18], or based on mathematical modelling of the alignment process [19], [20].

However, for the vertical assembly a problem of reducing interaction forces between the parts at the points of contact is still of relevance. These forces substantially increase when the angle between the axes decreases and approaches the value, when the three-point contact between a peg and a hole is replaced by the two-point contact.

There is another kind of devices recently been developed **technologically** and are in use for the assembly. In these devices, besides aligning motion characterized by the angle γ between the parts' axes, additional two rotating motions are transmitted to the peg. They are the motion about its own axis or about the axis of the hole. Practice indicates that it can reduce the forces of interaction between parts and helps to avoid seizure. For further improvement of such devices, to create a necessary control by computer programs, including training of AI, a theoretical justification of the assembly process is required. It should be based upon mechanical laws of the peg movement in the most general terms. There are only several publications where geometrical characteristics of compound motion are identified.

Works [21] and [22] present a mathematical model of the alignment of the parts with help of a device transmitting the vibration to a hole. Calculations presented in these papers define the position of the peg mass center relative to a vibrating hole. However, this model is insufficient to determine position of a peg as a solid body.

An assembly process involving the transmission of the rotating motion to the peg was studied in works [23], [24], [25]. Here the properties of a gyroscope, a body that has the only stationary point, are attributed to a peg. This attribution simplifies the calculations but it does not specify the dynamics of movement quite adequately.

Work [26] contains an analysis of aligning cylindrical parts, when both planar, and rotating motion about the hole axis are transmitted to a peg with the three-point contact between it and the aperture edge of vertically fixed hole. Dynamic Differential equations were written that enable to identify the basic patterns of this motion, and evaluate the effect, which rotating motion has on the alignment process.

While extending the study made in paper [26], this work is devoted to analyzing peg motion in the most general case, when the forces, acting on it, transfer all three types of movements allowed by connections: planar, rotation about hole axis, and rotation about its axis.

The work is aimed at addressing two major problems of the process for automated assembly of cylindrical parts:

- 1) determining the patterns of the peg movement ensuring the alignment of the parts when all three generalized coordinates (fig. 1) change: nutation angle $\gamma = \gamma(t)$, precession angle $\psi = \psi(t)$ and self-rotation angle $\varphi = \varphi(t)$;
- 2) determining the forces acting on the peg at the points of contact and preventing alignment of the parts. It allows to assess their effect on the process of the alignment, and to do it depending on motion patterns.

In the calculations of this paper, a peg and a hole are considered as solid bodies of a regular geometric shape with dimensions as follows: d – peg diameter, H – its height, D – diameter of a hole. At the beginning of alignment, angle between axes $\gamma > \arccos \frac{d}{D}$, that corresponds to contact of the parts at three points. One of the contact points K (Fig.1)

is placed between the shaft generating line and the hole aperture edge in the plane passing through the parts' axes, two other B_1 and B_2 are placed between the edges of both parts symmetrically to this plane.

Methodology and methods

Analysis of motion that enables alignment of a peg with a vertically fixed hole is based upon common patterns of mechanical movement of a solid body with the three degrees of freedom: nutation angle γ , precession angle ψ , and self-rotation angle φ .

All necessary characteristics of such motion might be obtained using differential equations of the mass center movement (1) and Lagrange differential equations (2).

$$m \frac{d^2 x_C}{dt^2} = \sum F_{kx}; \quad (1.1)$$

$$m \frac{d^2 y_C}{dt^2} = \sum F_{ky}; \quad (1.2) \quad (1)$$

$$m \frac{d^2 z_C}{dt^2} = \sum F_{kz}; \quad (1.3)$$

$$\frac{d}{dt} \frac{\partial T}{\partial \dot{\gamma}} - \frac{\partial T}{\partial \gamma} = Q_\gamma; \quad (2.1)$$

$$\frac{d}{dt} \frac{\partial T}{\partial \dot{\psi}} - \frac{\partial T}{\partial \psi} = Q_\psi; \quad (2.2) \quad (2)$$

$$\frac{d}{dt} \frac{\partial T}{\partial \dot{\varphi}} - \frac{\partial T}{\partial \varphi} = Q_\varphi. \quad (2.3)$$

The equations shall be compiled based on geometrical and kinematical patterns of the peg motion with the three degrees of freedom.

Left parts of the first three differential equations are the time derivatives from coordinates x_C, y_C, z_C of the peg mass center that are the functions of generalized coordinates γ, ψ, φ .

The peg position in the process of aligning is defined relative to the fixed system of coordinates O_1xyz (Fig. 1), the beginning of which coincides with center O_1 of the hole aperture edge, axis O_1z is directed along the hole axis, coordinate plane O_1xz passes through the hole axis and the peg axis in the initial position of the parts, axis O_1x is the line of intersection of this plane with the horizontal plane of the edge, it coincides with the hole diameter, axis O_1y is perpendicular to plane O_1xz .

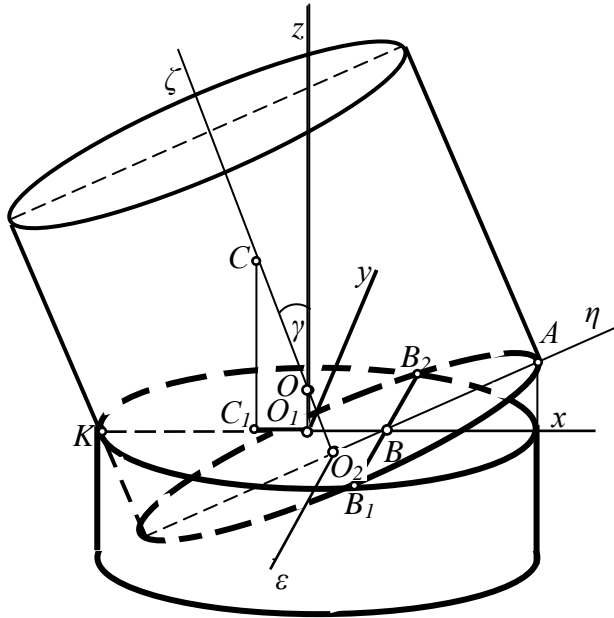


Fig. 1. Position of coordinate system $O_2\varepsilon\eta\zeta$ relative to system O_1xyz at the beginning of alignment

A moving coordinate system $O_2\varepsilon\eta\zeta$ (Fig. 1) is asso-

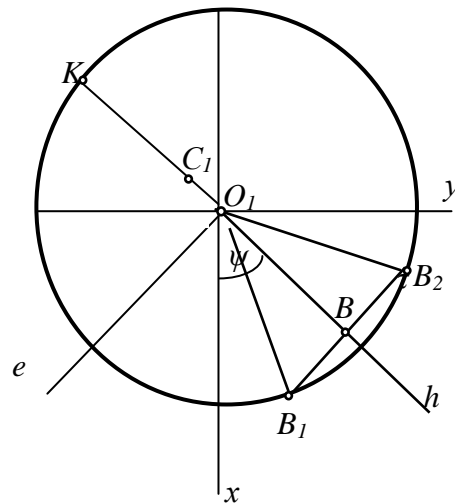


Fig. 2. Position of coordinate system O_1eh relative to fixed system O_1xy

ciated to the peg, with the beginning at the center of its aligned end, axis $O_2\zeta$ is directed along the peg axis, coordinate plane $O_2\zeta\eta$ passes through axes of the parts and is a principal plane of their symmetry in the course of alignment, axis $O_2\eta$ coincides with the diameter of a peg located in the plane of symmetry, axis $O_2\varepsilon$ is perpendicular to plane $O_2\zeta\eta$. In the peg moving, axis $O_2\varepsilon$ remains parallel to segment B_1B_2 , axis $O_2\eta$ remains perpendicular to this segment.

To define a position of the peg during its rotation about the axis of the sleeve, an auxiliary system of coordinates O_1ehz is used, with the beginning at point O_1 . Axis O_1h is a line of intersection of the parts' plane of symmetry with the horizontal plane of the hole and forms angle ψ with fixed axis O_1x . Axis O_1e is perpendicular to plane O_1hz (Fig. 2).

Coordinates of mass center relative to fixed system of coordinates O_1xyz , defined in work [26], are as follows:

$$\begin{aligned} x_C &= -O_1C_1 \cos \psi = -(0,5H - a_2) \sin \gamma \cos \psi = h_C \cos \psi; \\ y_C &= -O_1C_1 \sin \psi = -(0, H - a_2) \sin \gamma \sin \psi = h_C \sin \psi; \\ z_C &= (0,5H - a_2) \cos \gamma + a_1. \end{aligned} \tag{3}$$

where $a_1 = OO_1 = \frac{D - d \cos \gamma}{2 \sin \gamma}$ is a distance between point O of intersection of the parts' axes and center O_1 of

the hole edge circumference, and $a_2 = OO_2 = \frac{d - D \cos \gamma}{2 \sin \gamma}$ - distance between point O and center O_2 of the aligned peg end.

Since the peg axis intersects the hole axis at point O , the obtained values of mass center C coordinates enable to specify the equation of the peg axis depending on the generalized coordinates

$$\frac{x - x_O}{x_C - x_O} = \frac{y - y_O}{y_C - y_O} = \frac{z - z_O}{z_C - z_O};$$

where $x_O = 0$; $y_O = 0$; $z_O = a_1$ - coordinates of point O of the hole axis and peg intersection. Thus, the equation of the peg axis relative to a fixed system of coordinates shall be transformed as follows:

$$\frac{x}{x_C} = \frac{y}{y_C} = \frac{z - a_1}{z_C - a_1}. \tag{4}$$

The obtained values of the peg mass center coordinates (3) allow to transform the left parts of differential equations of the mass center movement (1)

$$\frac{d^2 x_C}{dt^2} = \frac{d\eta_C}{d\gamma} \cos \psi \dot{\gamma} - \eta_C \sin \psi \ddot{\psi} + \frac{d^2 \eta_C}{d\gamma^2} \cos \psi \dot{\gamma}^2 - \eta_C \cos \psi \dot{\gamma}^2 - 2 \frac{d\eta_C}{d\gamma} \sin \psi \dot{\gamma} \dot{\psi}; \tag{5.1}$$

$$\frac{d^2 y_C}{dt^2} = \frac{d\eta_C}{d\gamma} \sin \psi \dot{\gamma} + \eta_C \cos \psi \ddot{\psi} + \frac{d^2 \eta_C}{d\gamma^2} \sin \psi \dot{\gamma}^2 - \eta_C \sin \psi \dot{\gamma}^2 + 2 \frac{d\eta_C}{d\gamma} \cos \psi \dot{\gamma} \dot{\psi}; \tag{5.2} \tag{5}$$

$$m \frac{d^2 z_C}{dt^2} = m \left(\frac{d^2 z_C}{d\gamma^2} \dot{\gamma}^2 + \frac{dz_C}{d\gamma} \ddot{\gamma} \right). \tag{5.3}$$

The left parts of Lagrange equations shall be obtained through transforming kinetic peg energy, equal to the sum of kinetic energies of planar motion that is characterized by angle of nutation γ , peg rotation about its axis $O_2\zeta$ and rotation about hole axis O_1z , defined by angles of self-rotation ϕ and precession ψ ,

$$T = \frac{mV_C^2}{2} + \frac{I_{C\varepsilon} \dot{\gamma}^2}{2} + \frac{I_z \dot{\psi}^2}{2} + \frac{I_\zeta \dot{\phi}^2}{2}, \tag{6}$$

where m is a mass of a peg, V_C is a velocity of its mass center, $\dot{\gamma}$ is an angular velocity of planar motion, $\dot{\psi}$ - angular velocity of rotation motion of the peg about the hole axis, $\dot{\phi}$ angular velocity of self-rotation, $I_{C\varepsilon}$ - inertia moment of the peg relative to axis $C\varepsilon$, passing through its mass center perpendicular to the parts' plane of symmetry. I_z is inertia moment of the peg relative to hole axis O_1z , I_ζ - inertia moment of the peg relative to figure rotation axis $O_2\zeta$.

Here, $I_{C\varepsilon} = \frac{m}{12} (3R^2 + H^2)$ - central moment of peg inertia relative to axis $C\varepsilon$, passing through the peg mass center perpendicular to its plane of symmetry,

$I_\zeta = \frac{mR^2}{2}$ - moment of the peg inertia relative to its axis $O_2\zeta$,

$I_z = I_{C\eta} \sin^2 \gamma + I_\zeta \cos^2 \gamma + m\eta_C^2$ - moment of the peg inertia relative to hole axis O_1z , which is a variable value that depends on the angle between axes γ .

Mass center velocity is expressed through its projections to fixed axes of coordinates O_1xyz

$$V_{Cx} = \frac{dx_C}{dt} = \frac{d\eta_C}{d\gamma} \cos \psi \dot{\gamma} - \eta_C \sin \psi \dot{\psi};$$

$$V_{Cy} = \frac{dy_C}{dt} = \frac{d\eta_C}{d\gamma} \sin \psi \dot{\gamma} + \eta_C \cos \psi \dot{\psi};$$

$$V_{Cz} = \frac{dz_C}{d\gamma} \dot{\gamma};$$

where values h_C and z_C are defined by expressions (3). Hence,

$$V_C^2 = \left(\frac{dx_C}{dt} \right)^2 + \left(\frac{dy_C}{dt} \right)^2 + \left(\frac{dz_C}{dt} \right)^2 = \left(\frac{d\eta_C}{d\gamma} \right)^2 + \left(\frac{dz_C}{d\gamma} \right)^2 \dot{\gamma}^2 + \eta_C^2 \dot{\psi}^2.$$

Then, kinetic energy (5) shall be as follows

$$T = \frac{m}{2} \left\{ \left(\frac{d\eta_C}{d\gamma} \right)^2 + \left(\frac{dz_C}{d\gamma} \right)^2 \right\} \dot{\gamma}^2 + \eta_C^2 \dot{\psi}^2 + \frac{I_{C\varepsilon} \dot{\gamma}^2}{2} + \frac{I_z \dot{\psi}^2}{2} + \frac{I_\zeta \dot{\phi}^2}{2}. \tag{7}$$

After kinetic energy is properly transformed, the left parts of Lagrange equations shall have the following values (8)

$$\frac{d}{dt} \frac{\partial T}{\partial \dot{\gamma}} - \frac{\partial T}{\partial \gamma} = m \left[\left(\frac{d\eta_C}{d\gamma} \right)^2 + \left(\frac{dz_C}{d\gamma} \right)^2 \right] \ddot{\gamma} + I_{C\varepsilon} \ddot{\gamma} + m \left(\frac{d\eta_C}{d\gamma} \frac{d^2 \eta_C}{d\gamma^2} + \frac{dz_C}{d\gamma} \frac{d^2 z_C}{d\gamma^2} \right) \dot{\gamma}^2 -$$

$$-[m(\frac{d\eta_c}{d\gamma} \frac{d^2\eta_c}{d\gamma^2} + 0,5 \frac{dI_z}{d\gamma})\dot{\psi}^2]; \tag{8.1}$$

$$\frac{d}{dt} \frac{\partial T}{\partial \dot{\psi}} - \frac{\partial T}{\partial \psi} = (m\eta_c^2 + I_z)\ddot{\psi} + \frac{dI_z}{d\gamma} \dot{\gamma}\dot{\psi}; \tag{8.2} \tag{8}$$

$$\frac{d}{dt} \frac{\partial T}{\partial \dot{\phi}} - \frac{\partial T}{\partial \phi} = I_\zeta \frac{d^2\phi}{dt^2}. \tag{8.3}$$

The right parts of differential equations of mass center motion (1.1), (1.2), (1.3) shall be the sums of projections to fixed axes of coordinates of all forces that acts upon the peg, namely, assembling forces, peg gravity force and normal reactions and friction forces applied at the contact points.

Assembling forces for aligning parts are known values that depend on a method of assembly and assembly device used. Normal reactions and friction forces characterizing interaction forces between the parts shall be defined.

Directions of normal reactions shall be defined by location of contact points, and the value of each contact point depends on common patterns of motion. Normal reaction \bar{N}_K is directed perpendicular to the peg generating line; its projections to the fixed coordinate axes are equal to

$$N_{Kx} = N_K \cos \gamma \cos \psi; \quad N_{Ky} = N_K \cos \gamma \sin \psi; \quad N_{Kz} = N_K \sin \gamma. \tag{9}$$

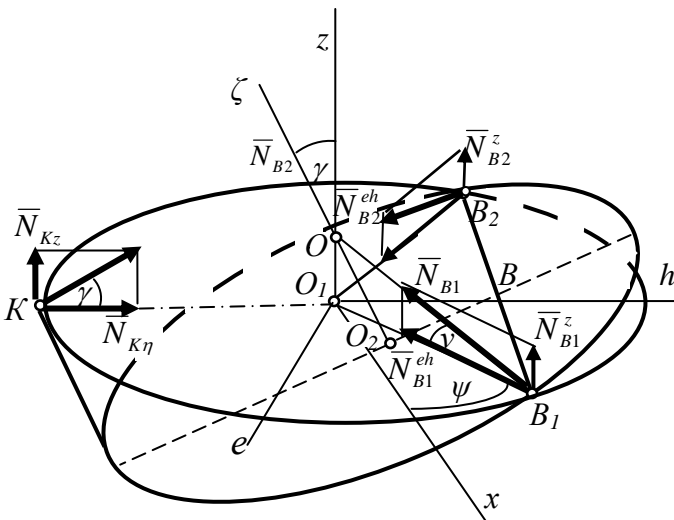


Fig. 3. Projections of normal reactions to horizontal plane

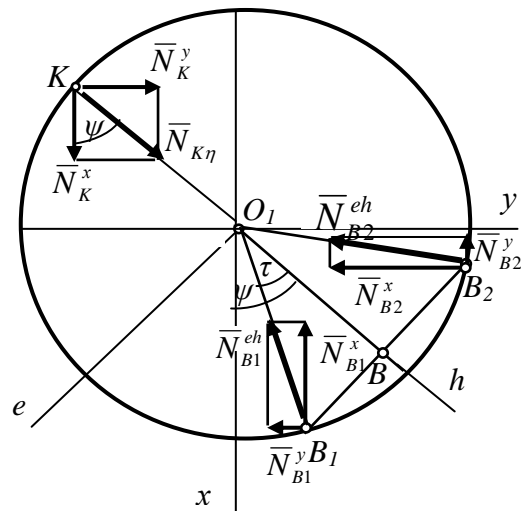


Fig.4. Projections of normal reactions to axes O1x and O1y

Lines of action of normal reactions \bar{N}_{B1} , \bar{N}_{B2} in symmetric points of contact B_1 and B_2 pass through point O of peg and hole axes intersection [26], and their direction cosines shall be defined from geometrical ratios. They should have the following values after transformations:

$$\begin{aligned} \cos \alpha_{B1}^N &= -\left(\frac{S_1 \cos \psi + b \sin \psi}{B_1}\right); & \cos \alpha_{B2}^N &= -\left(\frac{S_1 \cos \psi - b \sin \psi}{B_1}\right); \\ \cos \beta_{B1}^N &= -\left(\frac{S_1 \sin \psi - b \cos \psi}{B_1}\right); & \cos \beta_{B2}^N &= -\left(\frac{S_1 \sin \psi + b \cos \psi}{B_1}\right); \\ \cos \lambda_{B1}^N &= \frac{a_1}{B_1}; & \cos \gamma_{B2}^N &= \frac{a_1}{B_1}; \end{aligned}$$

where (Fig. 3) $b = BB_1 = BB_2$; $B_1 = OB_1 = OB_2 = \sqrt{0,25D^2 + a_1^2}$.

Hence, projections of normal reactions shall be written as follows

$$\begin{aligned}
 N_{B1}^x &= N_{B1} \cos \alpha_{B1}^N; & N_{B2}^x &= N_{B2} \cos \alpha_{B2}^N; & N_K^x &= N_K \cos \alpha_K^N; \\
 N_{B1}^y &= N_{B1} \cos \beta_{B1}^N; & N_{B2}^y &= N_{B2} \cos \beta_{B2}^N; & N_K^y &= N_K \cos \beta_K^N; \\
 N_{B1}^z &= N_{B1} \cos \lambda_{B1}^N; & N_{B2}^z &= N_{B2} \cos \lambda_{B2}^N; & N_K^z &= N_K \cos \lambda_K^N.
 \end{aligned}
 \tag{10}$$

The direction of friction force is always opposite to the absolute velocity of the point of its application that involves determining the values of velocities of contact points of parts B_1 , B_2 and K .

An absolute velocity of each point of the peg shall be equal to the sum of velocities of all components of the motions

$$\vec{V} = \vec{V}^\gamma + \vec{V}^\psi + \vec{V}^\phi;$$

where \vec{V}^γ - velocity of planar motion, \vec{V}^ψ and \vec{V}^ϕ - rotation velocities of points about hole and peg axes, respectively.

Hence, a direction of each velocity component at all points of parts' contact shall be determined.

Planar motion. When only one angle γ changes, the peg makes planar motion characterized by motion of its section $AEDN$ in the plane of symmetry. Velocities of the peg points located in the symmetry plane shall be defined [26] as rotatory around instantaneous velocity center L , located at the point of intersection of perpendicular lines to velocities \vec{V}_K and \vec{V}_A (Fig. 5). Velocities of symmetric points of contact B_1 and B_2 are equal to point B velocity, since they are located on one perpendicular line to the symmetry plane, passing through point B , hence, the values of the contact points' velocities shall be equal.

$$V_{B1}^\gamma = V_{B2}^\gamma = V_B^\gamma = BL\dot{\gamma}; \quad V_K^\gamma = KL\dot{\gamma}.$$

Projections of velocities \vec{V}_{B1}^γ , \vec{V}_{B2}^γ , \vec{V}_K^γ of points B_1 , B_2 and K on movable axes $O_2\eta$ and $O_2\zeta$ are equal to (Fig. 5)

$$\begin{aligned}
 V_{B1\eta}^\gamma &= V_{B2\eta}^\gamma = -BL\dot{\gamma} \cos \varepsilon_2 = -2a_2\dot{\gamma}; \\
 V_{B1\zeta}^\gamma &= V_{B2\zeta}^\gamma = -BL\dot{\gamma} \sin \varepsilon_2 = -2S_2\dot{\gamma}. \\
 V_{K\zeta}^\gamma &= KL\dot{\gamma}; \quad V_{K\eta}^\gamma = 0.
 \end{aligned}
 \tag{11}$$

Projections of these velocities \vec{V}_{B1}^γ , \vec{V}_{B2}^γ , \vec{V}_K^γ to auxiliary axis O_1h are equal (Fig.6)

$$V_{B1h}^\gamma = V_{B2h}^\gamma = -BL\dot{\gamma} \cos \varepsilon_1 = -2a_1\dot{\gamma}; \quad V_{Kh}^\gamma = -KL\dot{\gamma} \sin \gamma.
 \tag{12}$$

These expressions include (Fig.5) ε_1 – angle between segment BL and axis of hole, ε_2 – angle between segment BL and

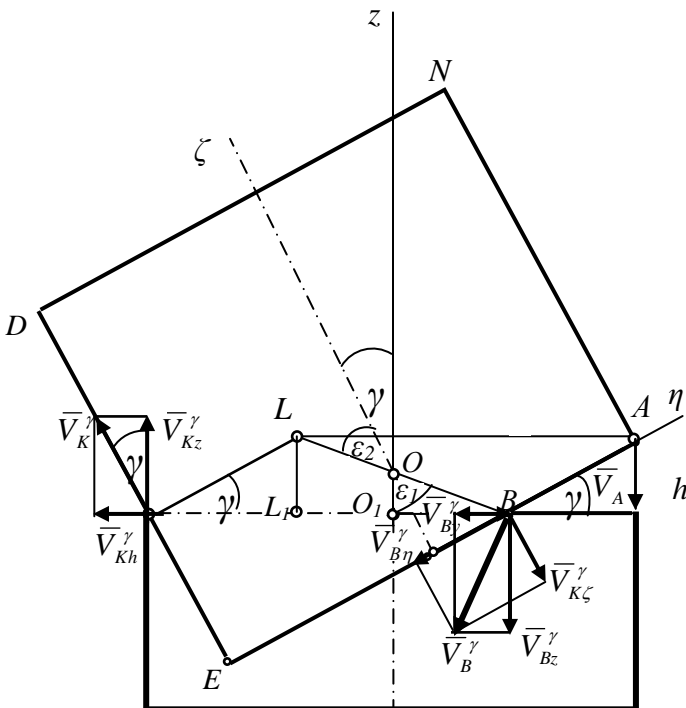


Fig. 5. Projections of velocities of planar motion on axis O_1y , O_1z and $O_2\eta$, $O_2\zeta$.

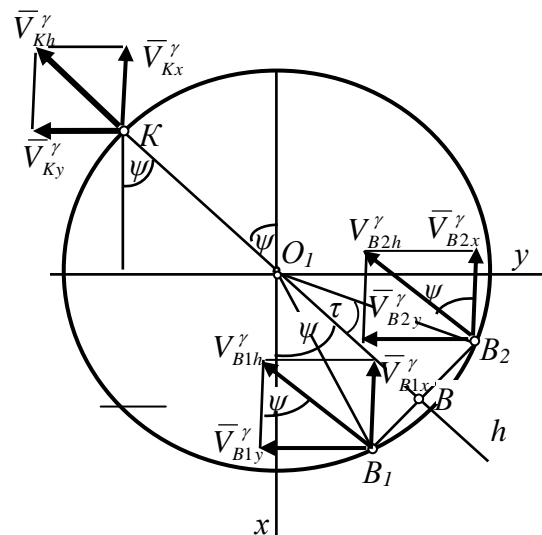


Fig.6. Projections of velocities of planar motion on fixed axes of coordinate system

peg axis, $\cos \varepsilon_1 = \frac{a_1}{OB}$; $\sin \varepsilon_1 = \frac{S_1}{OB}$; $\sin \varepsilon_2 = \frac{S_2}{OB}$;

$\cos \varepsilon_2 = \frac{a_2}{OB}$; $B = OB = \sqrt{a_1^2 + S_1^2} = \sqrt{a_2^2 + S_2^2}$; $BL = 2OB = 2B$.

Projections of velocities \bar{V}_{B1}^γ , \bar{V}_{B2}^γ , \bar{V}_K^γ to fixed axes O_1x , O_1y and O_1z (Fig. 6) are equal

$$\begin{aligned} V_{B1x}^\gamma &= V_{B2x}^\gamma = -V_{B1h}^\gamma \cos \psi = -2a_1 \cos \psi \dot{\gamma}; & V_{Kx}^\gamma &= -KL \sin \gamma \cos \psi \dot{\gamma}; \\ V_{B1y}^\gamma &= V_{B2y}^\gamma = -V_{B1h}^\gamma \sin \psi = -2a_1 \sin \psi \dot{\gamma}; & V_{Ky}^\gamma &= -KL \sin \gamma \sin \psi \dot{\gamma}; \\ V_{B1z}^\gamma &= V_{B2z}^\gamma = -2S_1 \dot{\gamma}. & V_{Kz}^\gamma &= KL \dot{\gamma} \cos \gamma. \end{aligned} \tag{13}$$

Rotation about hole axis occurs with angular velocity of $\dot{\psi} = \frac{d\psi}{dt}$. Velocities of contact points in this movement are located in the fixed plane O_1xy , directed (Fig.7) at tangents to the hole aperture edge circumference and at all contact points are equal in magnitude

$$V_{B1}^\psi = V_{B2}^\psi = V_K^\psi = 0,5D \dot{\psi}.$$

Projections of these velocities to the fixed axes of coordinates O_1x и O_1y (Fig. 7) taking values of $\sin \tau = \frac{b}{0,5D}$ and

$\cos \tau = \frac{S_1}{0,5D}$ into account shall be transformed to the following form:

$$\begin{aligned} V_{B1x}^\psi &= -(S_1 \sin \psi - b \cos \psi) \dot{\psi}; & V_{B2x}^\psi &= -(S_1 \sin \psi + b \cos \psi) \dot{\psi}; & V_{Kx}^\psi &= 0,5D \sin \psi \dot{\psi}; \\ V_{B1y}^\psi &= (S_1 \cos \psi + b \sin \psi) \dot{\psi}; & V_{B2y}^\psi &= (S_1 \cos \psi - b \sin \psi) \dot{\psi}; & V_{Ky}^\psi &= -0,5D \cos \psi \dot{\psi}; \\ V_{B1z}^\psi &= 0; & V_{B2z}^\psi &= 0; & V_{Kz}^\psi &= 0. \end{aligned} \tag{14}$$

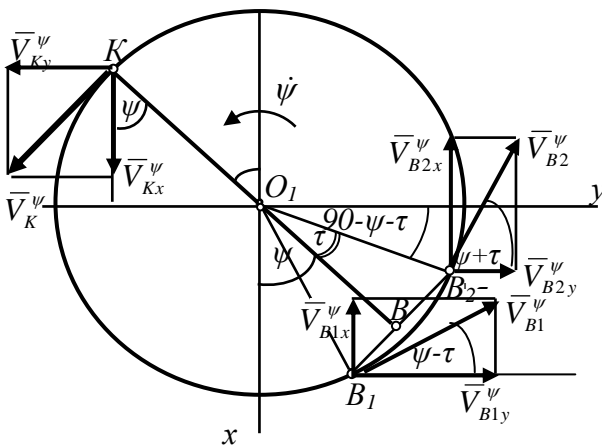


Fig.7. Projections of velocities of contact points when rotating about hole axis on axes O_1x and O_1y

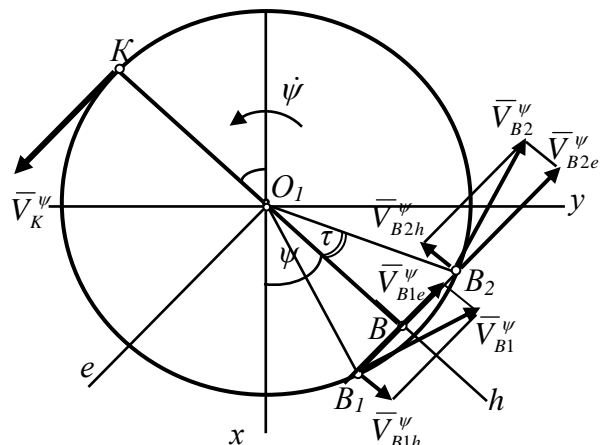


Fig. 8. velocities of contact points when rotating about hole axis on axes O_1e and O_1h .

To define projections of velocities \bar{V}_{B1}^ψ and \bar{V}_{B2}^ψ onto moving axes of coordinates $O_2\varepsilon$ and $O_2\eta$, they are first divided into two components. One of these components is parallel to axis O_1e , and the second one is parallel to axis O_1h (Fig. 8)

$$\bar{V}_{B1}^\psi = \bar{V}_{B1e}^\psi + \bar{V}_{B1h}^\psi; \quad \bar{V}_{B2}^\psi = \bar{V}_{B2e}^\psi + \bar{V}_{B2h}^\psi.$$

The values of these components define the projections of velocities to auxiliary axes O_2e and O_2h (Fig. 8)

$$V_{B1e}^\psi = -V_{B1}^\psi \cos \tau = -0,5D\dot{\psi} \frac{O_1B}{0,5D} = -S_1\dot{\psi}; \quad V_{B2e}^\psi = -V_{B2}^\psi \cos \tau = -0,5D\dot{\psi} \frac{O_1B}{0,5D} = -S_1\dot{\psi};$$

$$V_{B1h}^\psi = V_{B1}^\psi \sin \tau = 0,5D\dot{\psi} \frac{BB_1}{0,5D} = b\dot{\psi}; \quad V_{B2h}^\psi = -V_{B2}^\psi \sin \tau = -0,5D\dot{\psi} \frac{BB_2}{0,5D} = -b\dot{\psi}. \quad (15)$$

Components \bar{V}_{B1h}^ψ and \bar{V}_{B2h}^ψ , in its turn, shall be decomposed into two components, one of which is parallel to peg $O_2\zeta$ axis, the second is parallel to axis $O_2\eta$

$$\bar{V}_{B1h}^\psi = \bar{V}_{B1\zeta}^\psi + \bar{V}_{B1\eta}^\psi; \quad \bar{V}_{B2h}^\psi = \bar{V}_{B2\zeta}^\psi + \bar{V}_{B2\eta}^\psi.$$

Thus, velocities \bar{V}_{B1}^ψ and \bar{V}_{B2}^ψ of points B_1 and B_2 of rotation peg motion around hole O_1z axis shall be decomposed into three components

$$\bar{V}_{B1}^\psi = \bar{V}_{B1\varepsilon}^\psi + \bar{V}_{B1\zeta}^\psi + \bar{V}_{B1\eta}^\psi; \quad \bar{V}_{B2}^\psi = \bar{V}_{B2\varepsilon}^\psi + \bar{V}_{B2\zeta}^\psi + \bar{V}_{B2\eta}^\psi.$$

Projections of velocities \bar{V}_{B1}^ψ , \bar{V}_{B2}^ψ and \bar{V}_K^ψ to moving axes of coordinates $O_1\varepsilon$, $O_1\eta$ and $O_1\zeta$ shall be obtained through adding projections of their components (Fig. 8)

$$V_{B1\varepsilon}^\psi = V_{B1e}^\psi = -S_1\dot{\psi}; \quad V_{B2\varepsilon}^\psi = V_{B2e}^\psi = -S_1\dot{\psi}; \quad V_{K\varepsilon}^\psi = 0,5D\dot{\psi};$$

$$V_{B1\eta}^\psi = V_{B1h}^\psi \cos \gamma = b\dot{\psi} \cos \gamma; \quad V_{B2\eta}^\psi = V_{B2h}^\psi \cos \gamma = -b\dot{\psi} \cos \gamma; \quad V_{K\eta}^\psi = 0;$$

$$V_{B1\zeta}^\psi = -V_{B1h}^\psi \sin \gamma = -b\dot{\psi} \sin \gamma; \quad V_{B2\zeta}^\psi = V_{B2h}^\psi \sin \gamma = b\dot{\psi} \sin \gamma. \quad V_{K\zeta}^\psi = 0. \quad (16)$$

Rotation of peg about its axis occurs with angular velocity $\dot{\varphi} = \frac{d\varphi}{dt}$.

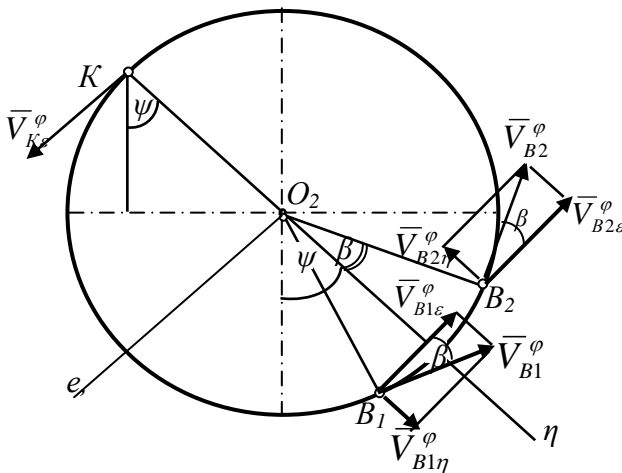


Fig. 9. Projections of self-rotation velocities to moving axes $O_2\varepsilon$ and $O_2\eta$

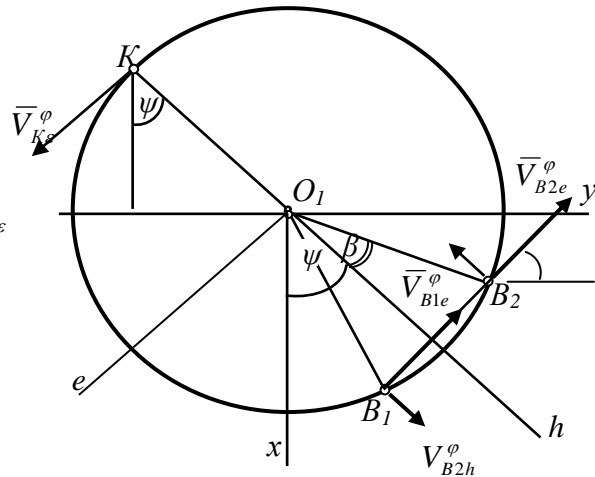


Fig. 10 Projections of self-rotation velocities to axes O_1e and O_1h

Velocities \bar{V}_K^φ , \bar{V}_{B1}^φ , \bar{V}_{B2}^φ of contact points K , B_1 and B_2 while moving are located in the plane of aligned peg end $O_2\varepsilon\eta$, and are equal in magnitude:

$$V_K^\varphi = V_{B1}^\varphi = V_{B2}^\varphi = 0,5d\dot{\varphi}.$$

Projections of these velocities to peg $O_2\zeta$ axis are equal to zero:

$$V_{B1\zeta}^\varphi = V_{B2\zeta}^\varphi = V_{K\zeta}^\varphi = 0.$$

Projections to moving axes $O_2\varepsilon$ and $O_2\eta$ (Fig.9) are equal to

$$V_{B1\varepsilon}^\varphi = V_{B1}^\varphi \cos \beta = -0,5d\dot{\varphi} \frac{S_2}{0,5d} = -S_2\dot{\varphi}; \quad V_{B1\eta}^\varphi = V_{B1}^\varphi \sin \beta = 0,5d\dot{\varphi} \frac{b}{0,5d} = b\dot{\varphi}.$$

$$V_{B2\varepsilon}^\varphi = -V_{B1}^\varphi \cos \beta = -0,5d\dot{\varphi} \frac{S_2}{0,5d} = -S_2\dot{\varphi}; \quad V_{B2\eta}^\varphi = V_{B1}^\varphi \sin \beta = -0,5d\dot{\varphi} \frac{b}{0,5d} = -b\dot{\varphi}.$$

$$V_{K\varepsilon}^\varphi = 0,5d\dot{\varphi}; \quad V_{K\eta}^\varphi = 0. \quad (17)$$

Each of $\bar{V}_{B1\eta}^\varphi$ and $\bar{V}_{B2\eta}^\varphi$ shall be divided into two components, one of which is directed along axis O_1h , the other is parallel to axis O_1z (Fig.10)

$$\bar{V}_{B1\eta}^\varphi = \bar{V}_{B1h}^\varphi + \bar{V}_{B1z}^\varphi; \quad \bar{V}_{B2\eta}^\varphi = \bar{V}_{B2h}^\varphi + \bar{V}_{B2z}^\varphi.$$

Hence, velocity in each point may be presented as a sum of three components, two of which are located in horizontal plane O_1xy (Fig.13), and the third one is located vertically, i.e. parallel to axis O_1z

$$\bar{V}_{B1}^\varphi = \bar{V}_{B1e}^\varphi + \bar{V}_{B1h}^\varphi + \bar{V}_{B1z}^\varphi; \quad \bar{V}_{B2}^\varphi = \bar{V}_{B2e}^\varphi + \bar{V}_{B2h}^\varphi + \bar{V}_{B2z}^\varphi;$$

Projections of rotation velocities of the points to auxiliary axis O_1h are equal to

$$V_{B1h}^\varphi = V_{B1\eta}^\varphi \cos \gamma = b \cos \gamma \dot{\varphi}; \quad V_{B2h}^\varphi = V_{B2\eta}^\varphi \cos \gamma = -b \cos \gamma \dot{\varphi}; \quad V_{Kh}^\varphi = 0; \quad (18)$$

Projections of velocities \bar{V}_{B1}^φ , \bar{V}_{B2}^φ and \bar{V}_K^φ to fixed axes of coordinates (Fig.10), after modifications shall be transformed to the form (19)

$$V_{B1x}^\varphi = V_{B1h}^\varphi \cos \psi - V_{B1e}^\varphi \sin \psi = -(S_2 \sin \psi - b \cos \gamma \cos \psi) \dot{\varphi};$$

$$V_{B1y}^\varphi = V_{B1h}^\varphi \sin \psi + V_{B1e}^\varphi \cos \psi = (S_2 \cos \psi + b \cos \gamma \sin \psi) \dot{\varphi}; \quad (19.1)$$

$$V_{B1z}^\varphi = V_{B1\eta}^\varphi \sin \gamma = b \sin \gamma \dot{\varphi};$$

$$V_{B2x}^\varphi = -V_{B2h}^\varphi \cos \psi - V_{B2e}^\varphi \sin \psi = -(S_2 \sin \psi + b \cos \gamma \cos \psi) \dot{\varphi};$$

$$V_{B2y}^\varphi = -V_{B2h}^\varphi \sin \psi + V_{B2e}^\varphi \cos \psi = (S_2 \cos \psi - b \cos \gamma \sin \psi) \dot{\varphi}; \quad (19.2) \quad (19)$$

$$V_{B2z}^\varphi = V_{B2\eta}^\varphi \sin \gamma = -b \sin \gamma \dot{\varphi};$$

$$V_{Kx}^\varphi = 0,5d \sin \psi \dot{\varphi}; \quad V_{Ky}^\varphi = -0,5d \cos \psi \dot{\varphi}; \quad V_{Kz}^\varphi = 0. \quad (19.3)$$

Projections of absolute velocities of each point of contact to fixed axes of coordinates O_1x , O_1y and O_1z shall be defined as sums of projections of the velocities components based on equations (13), (14) and (19), and shall be transformed to form (20)

$$V_{B1x} = V_{B1x}^\gamma + V_{B1x}^\psi + V_{B1x}^\varphi = -2a_1 \cos \psi \dot{\gamma} - (S_1 \sin \psi - b \cos \psi) \dot{\psi} - (S_2 \sin \psi - b \cos \gamma \cos \psi) \dot{\varphi};$$

$$V_{B1y} = V_{B1y}^\gamma + V_{B1y}^\psi + V_{B1y}^\varphi = -2a_1 \sin \psi \dot{\gamma} + (S_1 \cos \psi + b \sin \psi) \dot{\psi} + (S_2 \cos \psi + b \cos \gamma \sin \psi) \dot{\varphi};$$

$$V_{B1z} = V_{B1z}^\gamma + V_{B1z}^\psi + V_{B1z}^\varphi = -2S_1 \dot{\gamma} + b \sin \gamma \dot{\varphi}; \quad (20.1)$$

$$V_{B2x} = V_{B2x}^\gamma + V_{B2x}^\psi + V_{B2x}^\varphi = -2a_1 \cos \psi \dot{\gamma} - (S_1 \sin \psi + b \cos \psi) \dot{\psi} - (S_2 \sin \psi + b \cos \gamma \cos \psi) \dot{\varphi};$$

$$V_{B2y} = V_{B2y}^\gamma + V_{B2y}^\psi + V_{B2y}^\varphi = -2a_1 \sin \psi \dot{\gamma} + (S_1 \cos \psi + b \sin \psi) \dot{\psi} + (S_2 \cos \psi - b \cos \gamma \sin \psi) \dot{\varphi};$$

(20)

$$V_{B2z} = V_{B2z}^\gamma + V_{B2z}^\psi + V_{B2z}^\varphi = -2S_1 \dot{\gamma} - b \sin \gamma \dot{\varphi}; \quad (20.2)$$

$$V_{Kx} = V_{Kx}^\gamma + V_{Kx}^\psi + V_{Kx}^\varphi = -KL \sin \gamma \cos \psi \dot{\gamma} + 0,5D \sin \psi \dot{\psi} + 0,5d \sin \psi \dot{\varphi};$$

$$V_{Ky} = V_{Ky}^\gamma + V_{Ky}^\psi + V_{Ky}^\varphi = -KL \sin \gamma \sin \psi \dot{\gamma} - 0,5D \cos \psi \dot{\psi} - 0,5d \cos \psi \dot{\varphi};$$

$$V_{Kz} = V_{Kz}^\gamma + V_{Kz}^\psi + V_{Kz}^\varphi = KL \dot{\gamma} \cos \gamma. \quad (20.3)$$

Projections of absolute velocities of contact points to moving axes of coordinates $O_2\varepsilon$ и $O_2\eta$ shall be determined based on equations (12), (15) and (18)

$$\begin{aligned}
 V_{B1\varepsilon} &= V_{B1\varepsilon}^\gamma + V_{B1\varepsilon}^\psi + V_{B1\varepsilon}^\phi = -S_1\dot{\psi} - S_2\dot{\phi}; \\
 V_{B1\eta} &= V_{B1\eta}^\gamma + V_{B1\eta}^\psi + V_{B1\eta}^\phi = -2a_2\dot{\gamma} + b\cos\gamma\dot{\psi} + b\dot{\phi}; \quad (21.1)
 \end{aligned}$$

$$\begin{aligned}
 V_{B2\varepsilon} &= V_{B2\varepsilon}^\gamma + V_{B2\varepsilon}^\psi + V_{B2\varepsilon}^\phi = S_1\dot{\psi} - S_2\dot{\phi}; \\
 V_{B2\eta} &= V_{B2\eta}^\gamma + V_{B2\eta}^\psi + V_{B2\eta}^\phi = -2a_2\dot{\gamma} - b\cos\gamma\dot{\psi} - b\dot{\phi}; \quad (21.2) \quad (21)
 \end{aligned}$$

$$\begin{aligned}
 V_{K\varepsilon} &= V_{K\varepsilon}^\gamma + V_{K\varepsilon}^\psi + V_{K\varepsilon}^\phi = 0,5D\dot{\psi} + 0,5d\dot{\phi}; \\
 V_{K\eta} &= V_{K\eta}^\gamma + V_{K\eta}^\psi + V_{K\eta}^\phi = 0. \quad (21.3)
 \end{aligned}$$

Projections of absolute velocities of contact points to auxiliary axis O_1h shall be determined based on equations (12), (15) and (18)

$$\begin{aligned}
 V_{B1h} &= V_{B1h}^\gamma + V_{B1h}^\psi + V_{B1h}^\phi = -2a_1\dot{\gamma} + b\dot{\psi} + b\cos\gamma\dot{\phi}; \\
 V_{B2h} &= V_{B2h}^\gamma + V_{B2h}^\psi + V_{B2h}^\phi = -2a_1\dot{\gamma} - b\dot{\psi} - b\cos\gamma\dot{\phi}; \\
 V_{Kh} &= V_{Kh}^\gamma + V_{Kh}^\psi + V_{Kh}^\phi = -KL\sin\gamma\dot{\gamma}. \quad (22)
 \end{aligned}$$

The obtained values of projections of points B_1 , B_2 and K velocities to axes of coordinates allow to identify directions of friction forces relative to the specified axes of coordinates using direction cosines that will be opposite in sign to direction cosines of the respective absolute velocities.

Direction cosines of friction forces (23) relative to fixed axes of coordinates shall be defined by the following expressions

$$\cos\alpha_{B1}^F = -\frac{V_{B1x}}{V_{B1}}; \quad \cos\alpha_{B2}^F = -\frac{V_{B2x}}{V_{B2}}; \quad \cos\alpha_K^F = -\frac{V_{Kx}}{V_K}; \quad (23.1)$$

$$\cos\beta_{B1}^F = -\frac{V_{B1y}}{V_{B1}}; \quad \cos\beta_{B2}^F = -\frac{V_{B2y}}{V_{B2}}; \quad \cos\beta_K^F = -\frac{V_{Ky}}{V_K}; \quad (23.2) \quad (23)$$

$$\cos\lambda_{B1}^F = -\frac{V_{B1z}}{V_{B1}}; \quad \cos\lambda_{B2}^F = -\frac{V_{B2z}}{V_{B2}}; \quad \cos\lambda_K^F = -\frac{V_{Kz}}{V_K}; \quad (21.3)$$

where $V = \sqrt{V_x^2 + V_y^2 + V_z^2}$ - modulus of velocity in the corresponding point.

Right parts of differential equations of mass center motion (1.1), (1.2), (1.3) are the sums of projections to fixed axes of coordinates of all forces that act upon the peg, namely, assembling forces, peg gravity force and normal reactions and friction forces applied at the contact points. Analysis showed directions of normal reactions with direction cosines determined using expressions (9) and (10), and direction of all friction forces with direction cosines relative to fixed axes determined using expressions (20). Thus, the right parts of differential equations of mass center motion

shall be written as (24), where $F_x^{c\phi}$, $F_y^{c\phi}$, $F_z^{c\phi}$ are projections of assembling forces to fixed axes of coordinates.

$$\begin{aligned}
 \sum F_{kx} &= \\
 &= F_x^{c\phi} + N_K(\cos\alpha_K^N + f\cos\alpha_K^F) + N_{B1}(\cos\alpha_{B1}^N + f\cos\alpha_{B1}^F) + N_{B2}(\cos\alpha_{B2}^N + f\cos\alpha_{B2}^F); \quad (24.1)
 \end{aligned}$$

$$\begin{aligned}
 \sum F_{ry} &= \\
 &= F_y^{c\phi} + N_K(\cos\beta_K^N + f\cos\beta_K^F) + N_{B1}(\cos\beta_{B1}^N + f\cos\beta_{B1}^F) + N_{B2}(\cos\beta_{B2}^N + f\cos\beta_{B2}^F); \quad (24.2)
 \end{aligned}$$

$$\begin{aligned}
 \sum F_{ry} &= -mg + F_z^{c\phi} + \\
 &+ N_K(\cos\beta_K^N + f\cos\beta_K^F) + N_{B1}(\cos\beta_{B1}^N + f\cos\beta_{B1}^F) + N_{B2}(\cos\beta_{B2}^N + f\cos\beta_{B2}^F). \quad (24.3)
 \end{aligned}$$

$$Q_\gamma = m_{Ll}(\bar{F}^{c\phi}) - mg[S_1 - (0,5H - a_2)\sin\gamma] + fN_K \frac{KL^2\dot{\gamma}}{V_K} + fN_{B1} \frac{BL^2\dot{\gamma} + 2a_1b\dot{\psi} - 2a_2b\dot{\phi}}{V_{B1}} + fN_{B2} \left(\frac{BL^2\dot{\gamma} + 2a_2b\dot{\phi} + 2a_1b\dot{\psi}}{V_{B2}} \right). \quad (28.1)$$

Generalized force Q_ψ in the second Lagrange equation is equal to the sum of moments of all these forces relative to the hole axis. Gravity force is parallel to the hole axis, normal reactions intersect it, thus, their moments are equal to zero.

Moment of assembling forces $m_z(\bar{F}^{as})$ depends on a method used for assembling.

Moment of each friction force shall be defined by formula

$$m_z(\bar{F}) = xF_y - yF_x;$$

where x and y are coordinates of contact points K, B_1, B_2 in fixed system coordinates O_1xyz (Fig.12), values of which after transformations are equal to

$$x_{B1} = S_1 \cos\psi + b \sin\psi;$$

$$x_{B2} = S_1 \cos\psi - b \sin\psi; \quad x_K = -0,5D \cos\psi;$$

$$y_{B1} = S_1 \sin\psi - b \cos\psi;$$

$$y_{B2} = S_1 \sin\psi + b \cos\psi; \quad y_K = -0,5D \sin\psi.$$

Projections of friction forces to fixed axes of coordinates shall be expressed through normal reactions in contact points

$$F_{B1x} = fN_{B1} \cos\alpha_{B1}^F; \quad F_{B2x} = fN_{B2} \cos\alpha_{B2}^F; \quad F_{Kx} = fN_K \cos\alpha_K^F;$$

$$F_{B1y} = fN_{B1} \cos\beta_{B1}^F; \quad F_{B2y} = fN_{B2} \cos\beta_{B2}^F; \quad F_{Ky} = fN_K \cos\beta_K^F;$$

where all direction cosines are defined by values (27).

After substituting all values and further transformations, moments of friction forces $\bar{F}_{B1}, \bar{F}_{B2}$ and \bar{F}_K relative to axis O_1z shall have the following values

$$m_z(\bar{F}_{B1}) = x_{B1}F_{B1y} - y_{B1}F_{B1x} = fN_{B1} \frac{2a_1b\dot{\gamma} - (S_1S_2 + b^2 \cos\gamma)\dot{\phi} - 0,25D^2\dot{\psi}}{V_{B1}};$$

$$m_z(\bar{F}_{B2}) = x_{B2}F_{B2y} - y_{B2}F_{B2x} = -fN_{B2} \frac{2a_1b\dot{\gamma} + (S_1S_2 + b^2 \cos\gamma)\dot{\phi} + 0,25D^2\dot{\psi}}{V_{B2}};$$

$$m_z(\bar{F}_K) = x_KF_{Ky} - y_KF_{Kx} = -fN_K \frac{0,25D^2\dot{\psi} + 0,25dD\dot{\phi}}{V_K}.$$

Hence, generalized force of the second Lagrange equation shall be brought to the following form

$$Q_\psi = m_z(\bar{F}^{as}) + m_z(\bar{F}_K) + m_L(\bar{F}_{B1}) + m_z(\bar{F}_{B2}) = m_z(\bar{F}^{c\phi}) + fN_{B1} \frac{2a_1b\dot{\gamma} - (S_1S_2 + b^2 \cos\gamma)\dot{\phi} - 0,25D^2\dot{\psi}}{V_{B1}} - fN_{B2} \frac{2a_1b\dot{\gamma} + (S_1S_2 + b^2 \cos\gamma)\dot{\phi} + 0,25D^2\dot{\psi}}{V_{B2}} - fN_K \frac{0,25D^2\dot{\psi} + 0,25dD\dot{\phi}}{V_K}. \quad (28.2)$$

Generalized force Q_θ of the third Lagrange equation is equal to the sum of moments of all forces applied to the peg relative to peg axis $O_2\zeta$. Moments of gravity force and normal reactions are equal to zero, since lines of their action intersect this axis. Moments of friction forces relative to peg axis $O_2\zeta$ shall be defined by formula

$$m_\zeta(F) = \varepsilon F_\eta - \eta F_\varepsilon.$$

Coordinates of contact points in moving system of coordinates $O_2\varepsilon\eta\zeta$ are equal to

$$\begin{aligned} \varepsilon_{B1} &= BB_1 = b; & \varepsilon_{B2} &= BB_2 = -b; & \varepsilon_K &= 0; \\ \eta_{B1} &= O_2B = S_2; & \varepsilon_{B2} &= BB_2 = -b; & \eta_K &= -0,5d. \end{aligned}$$

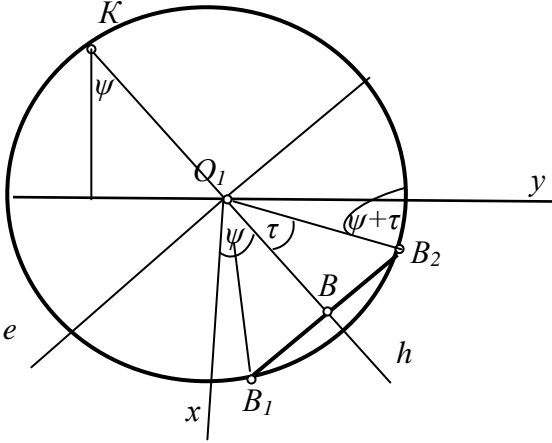


Fig.12. Position of contact points in coordinate system O_1xyz

Projections of friction forces are equal to

$$F_{B1\varepsilon} = fN_{B1} \cos \varepsilon_{B1}^F; \quad F_{B2\varepsilon} = fN_{B2} \cos \varepsilon_{B2}^F; \quad F_{K\varepsilon} = fN_K \cos \varepsilon_K^F;$$

$$F_{B1\eta} = fN_{B1} \cos \eta_{B1}^F; \quad F_{B2\eta} = fN_{B2} \cos \eta_{B2}^F; \quad F_{K\eta} = fN_K \cos \eta_K^F;$$

where direction cosines of friction forces with axes $O_2\varepsilon$ and $O_2\eta$, determined using values (23), (24), (25), are equal to

$$\cos \varepsilon_{B1}^F = \frac{S_1\dot{\psi} + S_2\dot{\phi}}{V_{B1}}; \quad \cos \eta_{B1}^F = \frac{2a_2\dot{\gamma} - b \cos \gamma \dot{\psi} - b\dot{\phi}}{V_{B1}}; \quad \cos \varepsilon_K^F = -\frac{0,5D\dot{\psi} + 0,5d\dot{\phi}}{V_K};$$

$$\cos \varepsilon_{B2}^F = \frac{S_1\dot{\psi} + S_2\dot{\phi}}{V_{B2}}; \quad \cos \eta_{B2}^F = \frac{2a_2\dot{\gamma} + b \cos \gamma \dot{\psi} + b\dot{\phi}}{V_{B2}}; \quad \cos \eta_K^F = 0;$$

After transformations, moments of friction forces relative to peg axis $O_2\zeta$ shall be brought to the following form

$$m_\zeta(F_K) = -fN_K \frac{0,25d^2\dot{\phi} + 0,25dD\dot{\psi}}{V_K};$$

$$m_\zeta(\bar{F}_{B1}) = fN_{B1} \frac{2a_1b\dot{\gamma} - 0,25d^2\dot{\phi} - (S_1S_2 + b^2 \cos \gamma)\dot{\psi}}{V_{B1}};$$

$$m_\zeta(\bar{F}_{B2})f = N_{B2} \frac{2a_1b\dot{\gamma} - 0,25d^2\dot{\phi} - (S_1S_2 + b^2 \cos \gamma)\dot{\psi}}{V_{B2}}.$$

Generalized force of the third Lagrange equation shall be as follows

$$Q_\varphi = m_\zeta(\bar{F}^{c\phi}) + fN_{B1} \frac{2a_1b\dot{\gamma} - 0,25d^2\dot{\phi} - (S_1S_2 + b^2 \cos \gamma)\dot{\psi}}{V_{B1}} +$$

$$+ fN_{B2} \frac{2a_1b\dot{\gamma} - 0,25d^2\dot{\phi} - (S_1S_2 + b^2 \cos \gamma)\dot{\psi}}{V_{B2}} - fN_K \frac{0,25d^2\dot{\phi} + 0,25dD\dot{\psi}}{V_K}; \quad (28.3)$$

where $m_\zeta(\bar{F}^{c\phi})$ is a moment of assembling force relative to peg axis $O_2\zeta$.

Comprehensive analysis of the peg motion enabled to define right (5) and left (28) parts of differential equations of mass center movement (1), and right (8) and left (28) parts of Lagrange equations (2). After equating corresponding values of these components, six differential equations shall be obtained (29)

$$m[(\frac{d\eta_C}{d\gamma})^2 + (\frac{dz_C}{d\gamma})^2] \ddot{\gamma} + I_{C\varepsilon} \ddot{\gamma} + m(\frac{d\eta_C}{d\gamma} \frac{d^2\eta_C}{d\gamma^2} + \frac{dz_C}{d\gamma} \frac{d^2z_C}{d\gamma^2}) \dot{\gamma}^2 - [m(\frac{d\eta_C}{d\gamma} \frac{d^2\eta_C}{d\gamma^2} + 0,5 \frac{dI_{Cz}}{d\gamma}) \dot{\psi}^2 +$$

$$+ (m\eta_C^2 + I_z) \ddot{\psi} + \frac{dI_z}{d\gamma} \dot{\gamma} \dot{\psi} = m_{Ll}(\bar{F}^{c\phi}) - mg[S_1 - (0,5H - a_2) \sin \gamma] +$$

$$+ fN_K \frac{KL^2 \dot{\gamma}}{V_K} + fN_{B1} [(fN_{B1} \frac{BL^2 \dot{\gamma} + 2a_1b\dot{\psi} - 2a_2b\dot{\phi}}{V_{B1}})] + fN_{B2} [\frac{BL^2 \dot{\gamma} + 2a_2b\dot{\phi} + 2a_1b\dot{\psi}}{V_{B2}}]. \quad (29.1)$$

$$(m\eta_C^2 + I_z) \ddot{\psi} + \frac{dI_z}{d\gamma} \dot{\gamma} \dot{\psi} = m_\zeta(\bar{F}^{c\phi}) - fN_K \frac{0,25D^2\dot{\psi} + 0,25dD\dot{\phi}}{V_K} +$$

$$+ fN_{B1} \frac{2a_1b\dot{\gamma} - (S_1S_2 + b^2 \cos \gamma)\dot{\phi} - 0,25D^2\dot{\psi}}{V_{B1}} - fN_{B2} \frac{2a_1b\dot{\gamma} + (S_1S_2 + b^2 \cos \gamma)\dot{\phi} - 0,25D^2\dot{\psi}}{V_{B2}}; \quad (29.2)$$

$$I_\zeta \ddot{\phi} = m_\zeta(\bar{F}^{c\phi}) - fN_K \frac{0,25d^2\dot{\phi} + 0,25dD\dot{\psi}}{V_K} + fN_{B1} \frac{2a_1b\dot{\gamma} - 0,25d^2\dot{\phi} - (S_1S_2 + b^2 \cos \gamma)\dot{\psi}}{V_{B1}} +$$

$$- fN_{B2} \frac{2a_1b\dot{\gamma} + 0,25d^2\dot{\phi} + (S_1S_2 + b^2 \cos \gamma)\dot{\psi}}{V_{B2}}. \quad (29.3)$$

$$m\left[\frac{d\eta_C}{d\gamma} \cos \psi \ddot{\gamma} - \eta_C \sin \psi \ddot{\psi} + \frac{d^2\eta_C}{d\gamma^2} \cos \psi \dot{\gamma}^2 - \eta_C \cos \psi \dot{\psi}^2 - 2\frac{d\eta_C}{d\gamma} \sin \psi \dot{\gamma} \dot{\psi}\right] = F_x^{c\phi} + N_K(\cos \alpha_K^N + f \cos \alpha_K^F) + N_{B1}(\cos \alpha_{B1}^N + f \cos \alpha_{B1}^F) + N_{B2}(\cos \alpha_{B2}^N + f \cos \alpha_{B2}^F); \quad (29.4)$$

$$m\left[\frac{d\eta_C}{d\gamma} \sin \psi \ddot{\gamma} + \eta_C \cos \psi \ddot{\psi} + \frac{d^2\eta_C}{d\gamma^2} \sin \psi \dot{\gamma}^2 - \eta_C \sin \psi \dot{\psi}^2 + 2\frac{d\eta_C}{d\gamma} \cos \psi \dot{\gamma} \dot{\psi}\right] = F_y^{c\phi} + N_K(\cos \beta_K^N + f \cos \beta_K^F) + N_{B1}(\cos \beta_{B1}^N + f \cos \beta_{B1}^F) + N_{B2}(\cos \beta_{B2}^N + f \cos \beta_{B2}^F); \quad (29.5)$$

$$m\left(\frac{d^2z_C}{d\gamma^2} \dot{\gamma}^2 + \frac{dz_C}{d\gamma} \ddot{\gamma}\right) = -mg + F_z^{c\phi} + N_K(\cos \lambda_K^N + f \cos \lambda_K^F) + N_{B1}(\cos \lambda_{B1}^N + f \cos \lambda_{B1}^F) + N_{B2}(\cos \lambda_{B2}^N + f \cos \lambda_{B2}^F) \quad (29.6)$$

This is a system of Dynamic Differential equations (29), and it is a mathematical model of process for aligning cylindrical parts in the most general way, when a peg, supported at the three points of the hole edge of vertically fixed hole, makes a compound motion characterized by three degrees of freedom. Such model may serve as a basis for considering all possible alternatives of vertical assembly schemes. A comparison of them will facilitate assessment of effect that rotatory motions have on reliability and quality of assembly.

Planar peg motion. that ensures a process of aligning parts occurs when one generalized coordinate, angle γ between axes of parts, changes. Such motion shall be performed when all assembling forces acting upon peg are brought to a plane system of forces in the symmetry plane of parts that is equivalent to one force \bar{F}^{as} and pair of forces with moment M_γ^{as} . Here, normal reactions and friction forces are equal in value $\bar{N}_{B1} = \bar{N}_{B2}$, $\bar{F}_{B1} = \bar{F}_{B2}$ in symmetrical contact points B_1 and B_2 ; their resultant forces \bar{N}_B and \bar{F}_B are applied in point B , the middle of segment B_1B_2 , and are located in the symmetry plane of parts (Fig.13).

Differential equations of motion of the peg with one degree of freedom shall be obtained by substituting values $\varphi = 0$, $\dot{\varphi} = 0$, $\psi = 0$, $\dot{\psi} = 0$ into system of equations (29) that shall be brought to form (30) after transformations made

$$m\left(\frac{dx_C}{d\gamma} \ddot{\gamma} + \frac{d^2x_C}{d\gamma^2} \dot{\gamma}^2\right) = F_x^{as} + N_K(\cos \gamma + f \sin \gamma) - 2N_{B1}(\sin \alpha \sin \varepsilon_1 - f \cos \varepsilon_1); \quad (30.1)$$

$$m\left(\frac{d^2z_C}{d\gamma^2} \dot{\gamma}^2 + \frac{dz_C}{d\gamma} \ddot{\gamma}\right) = F_z^{as} - mg + N_K(\sin \gamma - f \cos \gamma) + 2N_{B1}(\sin \alpha \cos \varepsilon_1 + f \sin \varepsilon_1); \quad (30.2)$$

$$m\left[\left(\frac{dx_C}{d\gamma}\right)^2 + \left(\frac{dz_C}{d\gamma}\right)^2\right] \ddot{\gamma} + m\left(\frac{dx_C}{d\gamma} \frac{d^2x_C}{d\gamma^2} + \frac{dz_C}{d\gamma} \frac{d^2z_C}{d\gamma^2}\right) \dot{\gamma}^2 + I_{Cx} \ddot{\gamma} = M_\gamma^{as} - mg[S_1 - (0,5H - a_2) \sin \gamma] - f N_K KL - 2f \dots \quad (30.3)$$

$$= M_\gamma^{as} - mg[S_1 - (0,5H - a_2) \sin \gamma] - f N_K KL - 2f \dots \quad (30.3)$$

Obtained equations (30) allow to specify, depending on a method for assembling, an equation of the peg motion $\gamma = \gamma(t)$, specify equation of the peg motion $\gamma = \gamma(t)$ that ensures alignment of parts, and values of dynamic reactions, which correspond to this

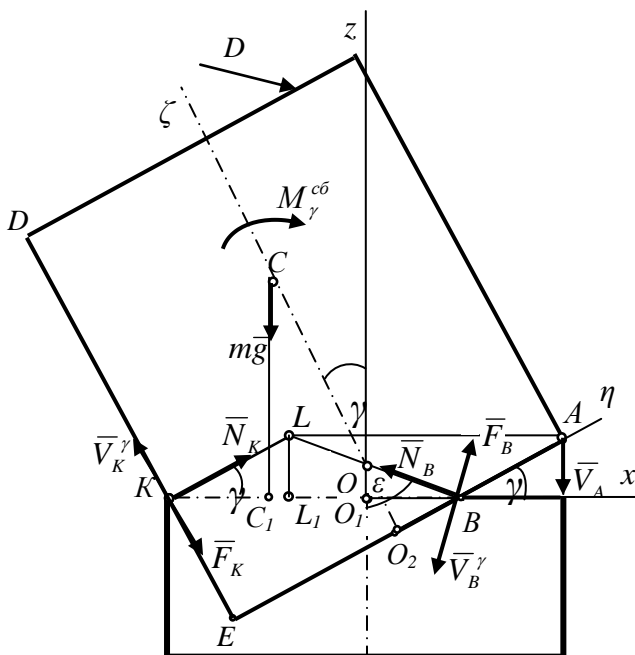


Fig. 13. Forces acting when plane-parallel motion occurs

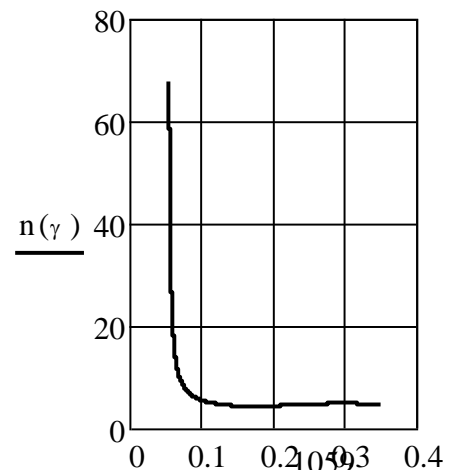


Fig. 14. Graph of reaction changing in point K when $\dot{\gamma} = 0,2$ 1/s

process. An algorithm for solving differential equations was compiled based on Mathcad package. Finally, it was found that interaction forces sharply increase irrespective of assembly method when angle between axes decreases, and reach maximum values when angle between axes approaches value $\gamma = \arccos d/D$, when contact of parts in three points is replaced by two-point contact.

By way of example, the results of analyzing the process of aligning parts when subjected to rotary moment M_γ^{as} , transmitting planar motion to the peg, are presented. Dynamic reactions in contact points were determined in graphic form for parts of $D = 50 \text{ mm}$, $d = 49,9 \text{ mm}$, $H = 70 \text{ mm}$. Friction coefficient shall be taken equal to $f = 0,2$. To simplify calculations, steady motion of the peg was chosen with angular velocity $\dot{\gamma} = 0,2 \text{ s}^{-1}$. Here, $\ddot{\gamma} = 0$, hence, two first equations (30.1) and (30.2) are sufficient to determine normal reactions

$$\begin{aligned} m \frac{d^2 x_C}{d\gamma^2} \dot{\gamma}^2 &= N_K (\cos \gamma + f \sin \gamma) - 2N_{B1} (\sin \alpha \sin \varepsilon_1 - f \cos \varepsilon_1); \\ m \frac{d^2 z_C}{d\gamma^2} \dot{\gamma}^2 &= -mg + N_K (\sin \gamma - f \cos \gamma) + 2N_{B1} (\sin \alpha \cos \varepsilon_1 + f \sin \varepsilon_1). \end{aligned} \quad (31)$$

Fig. 14 presents a graph showing relationship between angle γ and value $n_K = \frac{R_K}{mg}$, the ratio of overall reaction in

point K to the peg gravity force. Overall reaction \bar{R} in each point was determined as a geometrical sum of normal reaction \bar{N} and friction force \bar{F} , equivalent to $R_K = \sqrt{N_K^2 + F_K^2} = N_K \sqrt{1 + f^2}$. As it appears from the graph, when rotary moment M_γ^{as} (Fig.13) aligns parts, reaction \bar{R}_K in point K exceeds peg gravity force by more than 50 times during aligning and angle between axes approaching value $\gamma = \arccos(d/D)$.

To determine an impact of rotary motion of the peg around its axis on the process of aligning parts, differential equations of the peg motion with the two degrees of freedom: angle γ , characterizing planar motion, and self-rotation angle φ , specifying common patterns of the peg rotary motion around its axis, need to be written. Here, differential equations shall be obtained by substituting values $\psi = 0$, $\dot{\psi} = 0$ into equations (33). After all transformations five equations (36) were compiled that define common patterns of motion of the peg with the two degrees of motion, which enable to write equations of the peg motion and normal reactions in contact points depending on assembly forces applied.

$$\begin{aligned} m \left[\frac{d\eta_C}{d\gamma} \ddot{\gamma} + \frac{d^2 \eta_C}{d\gamma^2} \dot{\gamma}^2 \right] &= F_x^{as} + N_K (\cos \gamma + f \frac{KL \sin \gamma \dot{\gamma}}{V_K}) - \\ &- N_{B1} \left(\frac{S_1}{B_1} - f \frac{2a_1 \dot{\gamma} - b \cos \gamma \dot{\varphi}}{V_{B3}} \right) - N_{B2} \left(\frac{S_1}{B_1} - f \frac{2a_1 \dot{\gamma} + b \cos \gamma \dot{\varphi}}{V_{B2}} \right); \end{aligned} \quad (32.1)$$

$$N_{B1} \left(\frac{b}{B_1} - f \frac{S_2 \dot{\varphi}}{V_{B1}} \right) - N_{B2} \left(\frac{b}{B_1} + f \frac{S_2 \dot{\varphi}}{V_{B2}} \right) + f N_K \frac{0,5d\dot{\varphi}}{V_K} = 0; \quad (32.2)$$

$$\begin{aligned} m \left(\frac{dz_C}{d\gamma} \ddot{\gamma} + \frac{d^2 z_C}{d\gamma^2} \dot{\gamma}^2 \right) &= -mg + F_z^{as} + N_K (\sin \gamma - f \frac{KL \cos \gamma \dot{\gamma}}{V_K}) + \\ &+ N_{B1} \left(\frac{a_1}{B_1} + f \frac{2S_1 \dot{\gamma} - b \sin \gamma \dot{\varphi}}{V_{B1}} \right) + N_{B2} \left(\frac{a_1}{B_1} + f \frac{2S_1 \dot{\gamma} + b \sin \gamma \dot{\varphi}}{V_{B2}} \right); \end{aligned} \quad (32.3)$$

$$\begin{aligned} m \left[\left(\frac{d\eta_C}{d\gamma} \right)^2 + \left(\frac{dz_C}{d\gamma} \right)^2 \right] \ddot{\gamma} + I_{C\varepsilon} \ddot{\gamma} + m \left(\frac{d\eta_C}{d\gamma} \frac{d^2 \eta_C}{d\gamma^2} + \frac{dz_C}{d\gamma} \frac{d^2 z_C}{d\gamma^2} \right) \dot{\gamma}^2 &= m_{Ll} (\bar{F}^{as}) - \\ - mg [S_1 - (0,5H - a_2) \sin \gamma] + f N_K \frac{KL^2 \dot{\gamma}}{V_K} + f N_{B1} \left[(f N_{B1} \frac{BL^2 \dot{\gamma} - 2a_2 b \dot{\varphi}}{V_{B1}}) \right] + f N_{B2} \left[\frac{BL^2 \dot{\gamma} + 2a_2 b \dot{\varphi}}{V_{B2}} \right]; \end{aligned} \quad (32.4)$$

$$I_{\zeta} \ddot{\phi} = m_{\zeta} (\bar{F}^{as}) + fN_{B1} \frac{2a_1 b \dot{\gamma} - 0,25d^2 \dot{\phi}}{V_{B1}} - fN_{B2} \frac{2a_1 b \dot{\gamma} + 0,25d^2 \dot{\phi}}{V_{B2}}. \tag{32.5}$$

To compare values of dynamic reactions with the previous example, a process of alignment was considered, when both components of the peg motion occurred due to moments M_{LI}^{as} and M_{ϕ}^{as} acting upon it, creating motion with constant angular velocities: $\dot{\gamma} = 0,2 \text{ s}^{-1}$, $\dot{\phi} = 2 \text{ s}^{-1}$. Here, four differential equations may be adequate to determine reactions, as follows

$$m \frac{d^2 \eta_C}{d\gamma^2} \dot{\gamma}^2 = N_K (\cos \gamma + f \frac{KL \sin \gamma \dot{\gamma}}{V_K}) - N_{B1} (\frac{S_1}{B_1} - f \frac{2a_1 \dot{\gamma} - b \cos \gamma \dot{\phi}}{V_{B3}}) - N_{B2} (\frac{S_1}{B_1} - f \frac{2a_1 \dot{\gamma} + \cos \gamma \dot{\phi}}{V_{B2}}); \tag{33.1}$$

$$N_{B1} (\frac{b}{B_1} - f \frac{S_2 \dot{\phi}}{V_{B1}}) - N_{B2} (\frac{b}{B_1} + f \frac{S_2 \dot{\phi}}{V_{B2}}) + fN_K \frac{0,5d\phi}{V_K} = 0 \tag{33.2}$$

$$m \frac{dz_C}{d\gamma} \dot{\gamma} = -mg + N_K (\sin \gamma - f \frac{KL \cos \gamma \dot{\gamma}}{V_K}) + N_{B1} (\frac{a_1}{B_1} + f \frac{2S_1 \dot{\gamma} - b \sin \gamma \dot{\phi}}{V_{B1}}) + N_{B2} (\frac{a_1}{B_1} + f \frac{2S_1 \dot{\gamma} + b \sin \gamma \dot{\phi}}{V_{B2}}); \tag{33.3}$$

$$m (\frac{d\eta_C}{d\gamma} \frac{d^2 \eta_C}{d\gamma^2} + \frac{dz_C}{d\gamma} \frac{d^2 z_C}{d\gamma^2}) \dot{\gamma}^2 = M_{\gamma}^{c\phi} - mg[S_1 - (0,5H - a_2) \sin \gamma] + fN_K \frac{KL^2 \dot{\gamma}}{V_K} + fN_{B1} [(fN_{B1} \frac{BL^2 \dot{\gamma} - 2a_2 b \dot{\phi}}{V_{B1}}) + fN_{B2} [\frac{BL^2 \dot{\gamma} + 2a_2 b \dot{\phi}}{V_{B2}}]]; \tag{33.4}$$

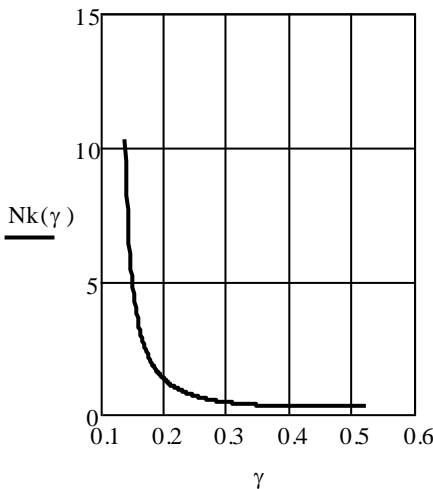


Fig. 15. Graph of changing reaction in point K when shaft rotates around its axis

The obtained equations were solved using Mathcad software for the parts with the same dimensions as when planar motion occurs.

Graph $n_K = n_K(\gamma)$, specifying relationship between angle γ and a ratio of overall reaction in point K to gravity force when peg rotates about its axis, is given in Fig. 15. As it follows from the graph, maximum value of this reaction is considerably lower than that, when rotation of a peg with one degree of freedom occurs, hence, rotation of a peg around its axis reduces interaction forces in contact points increasing thereby reliability and quality of the parts' assembly.

Differential equations, describing the process of aligning parts, involve friction forces as components. Hence, expressions for all required values, obtained as a result of solving these equations, depend on the value of friction coefficient that specifies all particular features of a certain method for assembly: dimensions, material, and quality of processing the parts.

Friction coefficient needs to be determined to increase accuracy of all calculations associated with computing forces applied to the peg in contact points. There are no recommendations about determining friction coefficient in the published theoretical studies of the process of aligning cylindrical parts; all studies specify friction

coefficient with no justification of selecting its value. Therefore, to improve accuracy of all calculations associated with aligning a peg and a hole, a problem of determining friction coefficient appropriate to certain parts and conditions of movement thereof is of relevance.

The determined common patterns of planar motion of a peg enable to experimentally identify the coefficient based on the results of alignment process. The peg gravity force may, depending on a position of mass center, facilitate or impede alignment of the parts, however, gravity force moment relative to instantaneous center of velocities is not sufficient to transmit alignment movement to a peg. Peg equilibrium with no assembly forces is possible in a certain range of angle γ values between axes of the parts. Here, a pattern of equilibrium and values of interaction forces in contact points depend not only on inclination angle, but also on a relative position of instantaneous center of velocities L and mass center of peg C, where gravity force is applied.

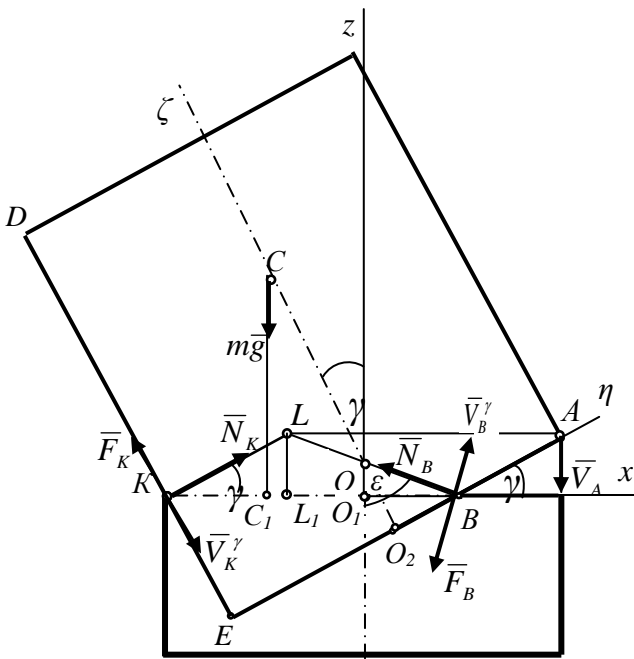


Fig. 16. Active forces when shaft stalling under action of gravity force

(34.1)

$$\sum F_{kz} = N_K (\sin \gamma + f \cos \gamma) + 2N_{B1} (\sin \alpha \cos \varepsilon - f \sin \varepsilon) - mg = 0; \quad (34.2)$$

$$\sum m_L(\bar{F}_K) = -mg \cdot h_{mg} - fN_K h_K - 2fN_B h_B = 0. \quad (34.3)$$

Normal reactions in the symmetrical contact points in these equations are equal in value: $N_{B1} = N_{B2}$, α – angle between segments B_1B_2 and OB_1 , $h_{mg} = C_1L_1 = (0,5H - a_2) \sin \gamma - S_1$; $h_K = KL$; $h_B = BL$.

To solve equations computer software "PTC Mathcad" was used. Thus, for parts fabricated from steel with hole diameter $D = 50 \text{ mm}$, clearance setting $\delta = 0,1 \text{ mm}$, peg height $H = 70 \text{ mm}$, angle γ when peg started to stall is equal to $0,33(20,06^\circ)$, and friction coefficient determined using equations (11) was equal to $f = 0,209$. For part of $H = 100 \text{ mm}$ height, $D = 50 \text{ mm}$, $\delta = 0,1 \text{ mm}$ stalling angle $\gamma = 0,27(41,04^\circ)$ that corresponded to $f = 0,2$.

Differential equations of planar motion (38) enable to determine reactions in contact points depending on the value of friction coefficient between parts in the course of their alignment. Reactions \bar{N}_K and \bar{N}_{B1} were identified based on these equations during assembling cylindrical parts of the following sizes: $D = 50 \text{ mm}$, $d = 49,9 \text{ mm}$, $H = 70 \text{ mm}$ for two values of friction coefficient between their surfaces, one of which $f_1 = 0,201$ corresponds to angle $\gamma_1 = 70^\circ$, the second $f_2 = 0,252$ corresponds to angle $\gamma_2 = 69^\circ$. In both cases alignment process was analyzed for steady motion when $\dot{\gamma} = 0,2 \text{ 1/s}$, $\ddot{\gamma} = 0$. For $f_2 = 0,252$ maximum value of reaction in point K exceeded 1.3 times the value of the same reaction for $f_1 = 0,201$. Hence, to increase accuracy of calculations when evaluating assembly devices, it is necessary to identify the value of pertinent friction coefficient.

Conclusions. A detailed kinematic analysis of a compound motion of the peg supported at the edge of vertically fixed hole was performed. In this analysis all three degrees of freedom in the course of alignment process were taken into account. The directions of the interaction forces were identified at the peg and hole contact points.

Dynamic Differential equations describing a process of aligning cylindrical parts were written. They depend on the relative position of the parts and acting forces between them. In these equations, the impact of the two rotary motions of the peg, around its axis and around axis of the hole, is taken into account, so they are considered in the most general case. According to the study, the friction coefficient is dependent on the position of the peg with the three-point contact at the hole aperture. A method for experimental determination of this friction coefficient was suggested in this paper. The material presented in this paper is a complete mathematical theory of mechanical movement of a quadric cylinder supported at the edge of a circular horizontal hole. It was developed using methods of theoretical mechanics. The theory enables to analyze all possible alternatives of vertical assembly, to determine interaction forces of parts at contact points, and to specify the impact of all parameters of the peg motion components on the alignment process.

When $O_1C_1 > O_1L_1$, gravity force moment impedes alignment of parts. When values $O_1C_1 < O_1L_1$ (Fig.16), gravity force creates a moment facilitating alignment process, however, according to practice, when vertical scheme of assembly is utilized, there are no values of angle γ , at which a peg would turn towards alignment of parts when subjected to only gravity force. Gravity force moment creates a stalling torque towards increasing angle γ , and peg motion under gravity is possible only towards increasing angle between parts' axes.

Beginning of stalling corresponds to the maximum value of friction coefficient in equilibrium.

To determine friction coefficient, a peg was installed on a hole edge under various angles, and angle γ was identified when the peg started to move towards its increasing. An inclination angle was determined for several pegs and holes fabricated from the same material. For experimentally identified value of angle γ , equations of peg equilibrium shall be written (34), with unknown normal reactions and friction coefficient in the alignment method in question (Fig. 15)

$$\sum F_{kx} =$$

$$N_K (\cos \gamma - f \sin \gamma) - 2N_{B1} (\sin \alpha \sin \varepsilon + f \cos \varepsilon) = 0;$$

The developed mathematical model of the peg compound motion may help to select parameters and modes of assembly, to design the assembly devices. Its major advantage lies in the increased technological potential of a robotized assembly, base either on classical computer modelling or supported AI training.

Discussion. In all the devices for Peg-in-Hole assembly, the angle between the peg and the hole is considered for their alignment. The devices take care about a decrease in this angle until the axes of the details are aligned, and the peg can be inserted into the hole. The process of simple alignment, however, can have undesirable effects and lead to the seizure of the parts. To overcome this effect, a certain kind of assembly devices has been widely developed and introduced into practice. In these devices the additional vibration motions are transmitted to either peg or hole, in addition to the planar alignment motion. These vibration motions reduce the interaction forces and, hence, increase the quality and reliability of the assembly.

In order to further develop and improve the process, the mathematical description of the alignment process, and attendant effects, could be of a significant importance. Unfortunately, the number of the publications, where this description was extensively considered is relatively low. Among the good examples are papers [21] and [22]. They mathematically consider the Peg-on-Hole alignment with vibration motion transmitted to a peg. The conditions, upon which the peg mass center approaches the sleeve axis are specified in this paper. The obtained mathematical model describes the alignment of the parts in two cases: with one- and two-point contact between the parts. The model specifies the coordinates of the peg mass center in the system. Unfortunately, the position of the mass center of the peg characterizes the relative position only partially, and cannot be used, for a three-point contact between the parts.

Works [23], [24], [25] cover the dynamics process of the high-speed rotation assembly. During this process, the high-speed rotation motion is transmitted to a peg about its vertical axis. The presented dynamic model of alignment process based upon gyroscope theory allows to define the time for alignment and the threshold for angular velocity. The computations given in these papers are incomplete since they do not determine interaction forces between parts and do not assess their impact on alignment process.

Paper [26] gives a comprehensive theoretical description of the peg compound motion with the two degrees of freedom. It overcame the limitations of the previously mentioned models. In that paper all kinematic characteristics, and directions of the interaction forces were determined. The model expressed in Dynamic Differential equations included the dependence of the motion parameters on the applied assembly forces as well as nutation and precession angles. It allowed to analyze the alignment process taking all these effects into account.

Current work extends the study of the previous paper. It takes all three generalized coordinates into account, and performs the kinematic and dynamic analyses of the peg motion in the most general case.

The presented material of this paper is the mathematical model of mechanical motion of the Peg-on-Hole alignment in the most general case. Use of this model can be of a great importance for the design of the assembly devices for the vertical Peg-in-Hole assembly. It helps to optimize the parameters regimes, and specifications for the already existing assembly devices. In addition, general theory could lead to the design of the new modes of assembly that were previously inaccessible due to limitations of the previous models. And as an acknowledgement for the digital era, the knowledge of the mathematics behind the assembly process simplifies the programming of Peg-in-Hole assembly devices, including classical control systems and training of Artificial Intelligence.